

# Deciphering the regulon of a GntR family regulator via transcriptome and ChIP-exo analyses and its contribution to virulence in *Xanthomonas citri*

XIAOFENG ZHOU†, QING YAN† AND NIAN WANG\*

Citrus Research and Education Center, Department of Microbiology and Cell Science, IFAS, University of Florida, 700 Experiment Station Road, Lake Alfred, FL 33850, USA

## SUMMARY

*Xanthomonas* contains a large group of plant-associated species, many of which cause severe diseases on important crops worldwide. Six gluconate-operon repressor (GntR) family transcriptional regulators are predicted in *Xanthomonas*, one of which, belonging to the YtrA subfamily, plays a prominent role in bacterial virulence. However, the direct targets and comprehensive regulatory profile of YtrA remain unknown. Here, we performed microarray and high-resolution chromatin immunoprecipitation-exonuclease (ChIP-exo) experiments to identify YtrA direct targets and its DNA binding motif in *X. citri* ssp. *citri* (*Xac*), the causal agent of citrus canker. Integrative microarray and ChIP-exo data analysis revealed that YtrA directly regulates three operons by binding to a palindromic motif GGTG-N<sub>16</sub>-CACC at the promoter region. A similar palindromic motif and YtrA homologues were also identified in many other bacteria, including *Stenotrophomonas*, *Pseudoxanthomonas* and *Frateuria*, indicating a widespread phenomenon. Deletion of *ytrA* in *Xac* abolishes bacterial virulence and induction of the hypersensitive response (HR). We found that YtrA regulates the expression of *hrp/hrc* genes encoding the bacterial type III secretion system (T3SS) and controls multiple biological processes, including motility and adhesion, oxidative stress, extracellular enzyme production and iron uptake. YtrA represses the expression of its direct targets in artificial medium or *in planta*. Importantly, over-expression of *yro3*, one of the YtrA directly regulated operons which contains *trmL* and *XAC0231*, induced weaker canker symptoms and down-regulation of *hrp/hrc* gene expression, suggesting a negative regulation in *Xac* virulence and T3SS. Our study has significantly advanced the mechanistic understanding of YtrA regulation and its contribution to bacterial virulence.

**Keywords:** bacterial virulence, ChIP-exo, GntR, microarray, type III secretion system, *Xanthomonas*.

## INTRODUCTION

Up to 10% of genes in the bacterial genome encode transcription factors (TFs) which can be grouped according to their type of DNA binding and conserved binding domain (Pabo and Sauer, 1992; Rodionov, 2007). The most studied group is helix–turn–helix (HTH) TFs which have a conserved DNA binding domain containing an  $\alpha$ -helix, a turn and a second  $\alpha$ -helix (Rigali *et al.*, 2002). The GntR family of TFs are named after the gluconate-operon repressor in *Bacillus subtilis* (Haydon and Guest, 1991) and are one of the most common TFs. GntR regulators contain a DNA binding HTH domain at the N-terminus of the protein and an effector binding and/or oligomerization (E-b/O) domain at the C-terminus. A conformation change occurs in the regulator on binding to an effector molecule, affecting the subsequent regulation of target genes. GntR usually forms a dimer and binds to two-fold symmetric DNA operator sequences (palindromic motif) so that each monomer recognizes a half-site (Konig *et al.*, 2009). The N-terminal DNA binding domain of GntR regulators is highly conserved, whereas the E-b/O domain at the C-terminus is diverse and heterogeneous (Rigali *et al.*, 2002; Vindal *et al.*, 2007). Based on the E-b/O domain topology and secondary structure, the GntR family can be divided into seven subfamilies, including AraR, DevA, FadR, HutC, MocR, PlmA and YtrA (Hoskisson and Rigali, 2009; Suvorova *et al.*, 2015; Vindal *et al.*, 2007).

Proteins in the YtrA subfamily possess a conserved HTH DNA binding domain, but a reduced E-b/O domain with only two  $\alpha$ -helices. The average length of the E-b/O domain in YtrA proteins is about 50 amino acids. Generally, *ytrA* is located at the beginning of a self-regulated operon encoding the ATP binding cassette (ABC) transport systems in several bacterial species (Rigali *et al.*, 2002; Salzberg *et al.*, 2011; Vindal *et al.*, 2007). In *B. subtilis*, YtrA responds to ramoplanin, a cell wall-targeted antibiotic, and thus is predicted to be a regulator of cell envelope stress responses (Salzberg *et al.*, 2011).

*Xanthomonas citri* ssp. *citri* (*Xac*) is an important bacterial pathogen that severely affects citrus production worldwide by causing citrus canker disease. Many virulence-associated factors contribute to the bacterial proliferation *in planta*, suppression of plant defences and symptom development, including extracellular polysaccharide (EPS) (Rigano *et al.*, 2007), lipopolysaccharide

\*Correspondence: Email: nianwang@ufl.edu

†These authors contributed equally to this work.

(LPS) (Casabuono *et al.*, 2011; Li and Wang, 2011), type II secretion system (T2SS) (Baptista *et al.*, 2010; Yan and Wang, 2012), type III secretion system (T3SS) and effectors (Dunger *et al.*, 2005; Laia *et al.*, 2009; Swarup *et al.*, 1992; Zhou *et al.*, 2015) and *rpf*-mediated quorum sensing system (Guo *et al.*, 2012). Among them, T3SS plays a critical role in bacterial infection in both plant and animal pathogens (Alfano and Collmer, 2004; Buttner, 2012; Buttner and He, 2009; Galan *et al.*, 2014). In *Xanthomonas*, T3SS is encoded by *hrp/hrc* genes and regulated by two key regulators, HrpG and HrpX. A putative cognate sensor kinase, named HpaS, phosphorylates HrpG during *Xanthomonas campestris* pv. *campestris* infection (Li *et al.*, 2014). The phosphorylation results in the activation of HrpG and up-regulation of HrpX which binds to a PIP (plant-inducible promoter) box conserved in the promoters of most *hrp/hrc* operons. YtrA has been reported to regulate bacterial virulence, the hypersensitive response (HR) and T3SS in *Xanthomonas campestris* pv. *campestris* (An *et al.*, 2011). However, the mechanistic understanding of YtrA regulation of its targets remains elusive.

Previously, we have identified a YtrA transcriptional regulator XAC1548 (named YtrA hereafter), which is a key regulator of bacterial virulence in *Xac*, through EZ-Tn5 transposon mutagenesis (Yan and Wang, 2012). In this study, we aim to probe the direct targets of YtrA and its binding motif. We employed microarray and chromatin immunoprecipitation-exonuclease (ChIP-exo) for such a purpose. The predicted YtrA binding motif and its interaction with YtrA were confirmed using electrophoretic mobility shift assay (EMSA). The regulation of YtrA was further investigated in the light of its involvement in virulence.

## RESULTS

### YtrA is crucial for *Xac* pathogenicity and HR induction

As reported previously (Yan and Wang, 2012), the EZ-Tn5 insertional mutant 414H4 of *ytrA* is a non-polar mutant and EZ-Tn5 does not affect the downstream genes of *ytrA*. To confirm the critical role of YtrA in bacterial virulence, a *ytrA* deletion mutant was generated by double-crossover recombination. The *ytrA* deletion mutant failed to cause canker pustules, whereas the wild-type strain induced typical canker symptoms (Fig. 1A). Ectopic expression of YtrA-FLAG (hereafter) in the *ytrA* mutant complemented the impaired bacterial virulence to the wild-type level. Expression of YtrA-Flag was confirmed by immunoblot (Fig. 1D). The bacterial population of the *ytrA* mutant in the plant is significantly lower ( $P < 0.01$ ) than that of the wild-type and complemented strains (Fig. 1B). The insertion mutant 414H4 (Yan and Wang, 2012) and the deletion mutant (Fig. 1A) showed the same phenotype and both could be complemented by the wild-type *ytrA*, confirming the critical role of YtrA in bacterial virulence. To test whether *ytrA* downstream genes are involved in virulence, XAC1547, XAC1546

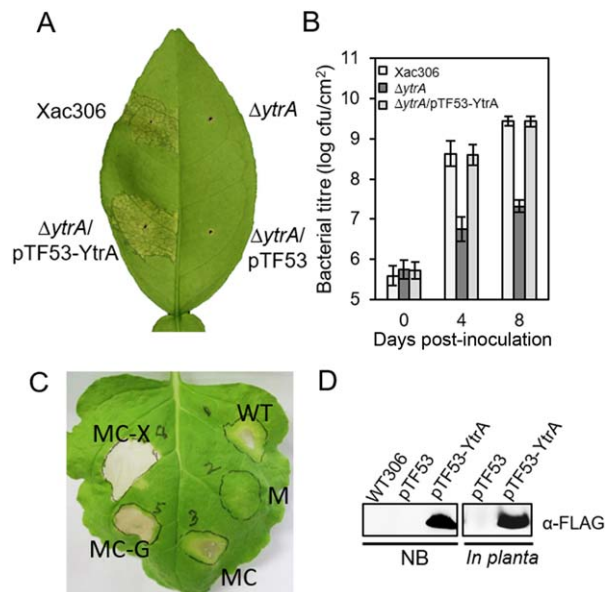


**Fig. 1** YtrA is crucial for *Xanthomonas citri* ssp. *citri* (*Xac*) virulence and for induction of the hypersensitive response (HR). (A) Bacterial pathogenicity on citrus plant. *Xac* wild-type, *ytrA* mutant ( $\Delta ytrA$ ), complementation strain ( $\Delta ytrA/pTF53-YtrA$ ) and *ytrA* mutant expressing the empty vector ( $\Delta ytrA/pTF53$ ) were infiltrated into citrus leaves at  $10^8$  colony-forming units (cfu)/mL. The leaves were photographed at 4 days post-inoculation (dpi). (B) Bacterial population in the plant. *Xac* cells were recovered from the inoculated leaves at 0, 4 and 8 dpi, and the values are the means of three repeats. Means  $\pm$  standard deviations are plotted. (C) HR induction on *Nicotiana benthamiana*. *Xac* strains were inoculated in tobacco [optical density at 600 nm ( $OD_{600}$ ) = 0.8]. WT, wild-type 306 with empty vector pUFR053; M, *ytrA* mutant with pUFR053; MC, *ytrA* mutant with complementary vector p53-YtrA; MC-X, *ytrA* mutant with p53-HrpX; MC-G, *ytrA* mutant with p53-HrpG. (D) Detection of protein expression from strain containing pTF53-YtrA in nutrient broth (NB) medium and *in planta*.

and XAC1545, which are located downstream of *ytrA*, were mutated. Mutation of XAC1547, XAC1546 and XAC1545 had no effect on bacterial virulence (Fig. S1, see Supporting Information). To test whether YtrA also contributes to HR induction, the wild-type, *ytrA* mutant and complemented strains were inoculated in the non-host plant tobacco. As shown in Fig. 1C, the *ytrA* mutant was deficient in HR induction. The deficiency in HR induction was restored by constitutive expression of YtrA in the mutant. These results indicate that YtrA is a key regulator of bacterial virulence and HR induction.

### Genome-wide transcriptional and binding profiles of YtrA

To experimentally identify YtrA regulated genes and binding sites, we first performed a whole-genome *Xac* oligonucleotide microarray analysis to obtain the regulatory profile of YtrA via comparison of the *ytrA* EZ-Tn5 mutant and wild-type strain. In addition,

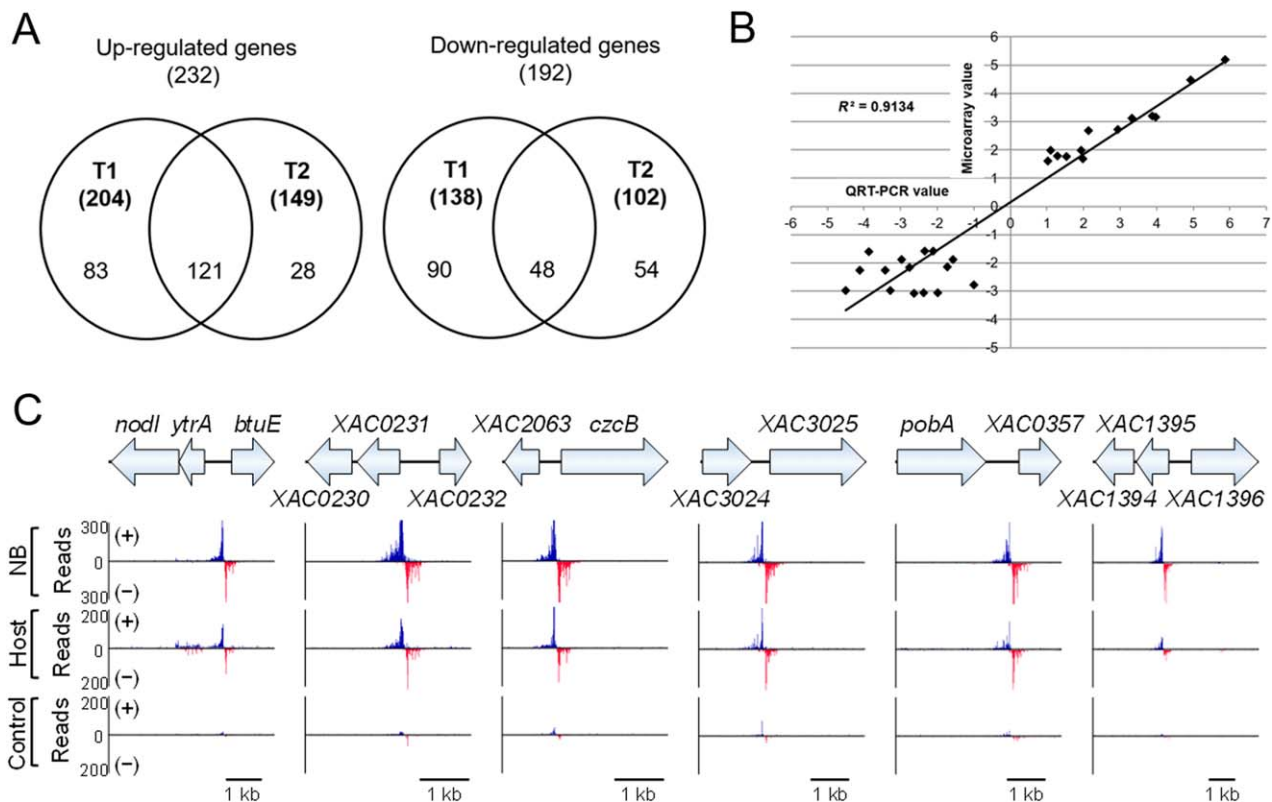


**Fig. 2** YtrA regulon and DNA binding sites. (A) Venn diagram shows the overlap of genes differentially regulated by YtrA at the two time points (T1, T2). (B) Validation of the microarray data by quantitative reverse transcription-polymerase chain reaction (QRT-PCR). The relative expression of 28 genes determined by microarray and QRT-PCR was compared. The  $R^2$  value is shown. (C) Six putative YtrA DNA binding sites identified by chromatin immunoprecipitation-exonuclease (ChIP-exo) experiments in nutrient broth (NB) and host plant. Strain expressing YtrA without a tag was used as a control. (+) (blue) and (-) (red) in ChIP-exo data indicate reads mapped on forward and reverse strands, respectively.

ChIP-exo was conducted to identify the YtrA DNA binding motif with near single-nucleotide resolution in medium and host (Rhee and Pugh, 2012).

To characterize the expression of the genes associated with the bacterial T3SS and other virulence-related traits that are not expressed in rich medium, a plant-mimic medium (XVM2 medium) was used to grow *Xac* for microarray assay. Two time points representing the middle exponential growth stage [T1, optical density at 600 nm ( $OD_{600}$ ) = 0.31] and the late exponential growth stage (T2,  $OD_{600}$  = 0.45) of *Xac* were selected. Based on the following cut-off with a false discovery rate (FDR) < 0.05 and absolute value of the  $\log_2$  fold change > 1.585 (equivalent to a fold change of 3.0), a total of 342 and 251 genes were differentially regulated by YtrA at T1 and T2, respectively (Fig. 2A). A total of 169 overlapping genes was identified in both T1 and T2 with a similar regulatory pattern (Table S1, see Supporting Information). Overall, the expression of 232 and 192 genes was up-regulated and down-regulated, respectively, in the *ytrA* mutant compared with the wild-type at both time points. To validate the microarray result, 15 down-regulated genes and 13 up-regulated genes were

selected for quantitative reverse transcription-polymerase chain reaction (QRT-PCR) analysis. The relative transcription ratios generated from microarray and QRT-PCR were compared. The QRT-PCR results are highly consistent with the microarray data with a coefficient of determination  $R^2 = 0.9134$  (Fig. 2B).

The genome-wide binding profile of YtrA was assessed using ChIP-exo. YtrA-Flag restored the deficient phenotype of the *ytrA* mutant, indicating that YtrA-Flag is fully functional and suitable for ChIP-exo experiments (Fig. 1). Peak-pairs were mapped to the *Xac* 306 genome and manually analysed. YtrA binds to its own promoter in *X. campestris* pv. *campestris* (An *et al.*, 2011). Consistently, we identified a strong peak-pair at the *ytrA* promoter region in *Xac* (Fig. 2C). The intensity of the peak-pair located at the *ytrA* promoter region was used as a reference for the identification of other peak-pairs. In total, six peak-pairs were identified, located at the promoter region of *ytrA* (XAC1548), XAC0231, *czcB* (XAC2064), XAC3025, XAC0357 and XAC1396 in rich medium (NB medium) and in host (Fig. 2C). A complementation strain without Flag-tag was used as a negative control. No peak was identified in the control.

### Combined ChIP-exo/microarray analysis reveals direct targets of YtrA and a conserved palindromic motif GGTG-N<sub>16</sub>-CACC

To identify direct targets of YtrA, the ChIP-exo data and YtrA transcriptome profile were compared. Three operons whose promoters interacted with YtrA (Fig. 2C) were also identified to be significantly

regulated by microarray at both time points (Fig. 3A, Table S1). Herein, we named the three operons *yro1* (YtrA regulated-operon 1) (including *ytrA*, *nodI*, *XAC1546*, *XAC1545*, *XAC1544* and *XAC1543*), *yro2* (including *czcB*, *XAC2065* and *XAC2066*) and *yro3* (including *XAC0231* and *XAC0230*) (Fig. 3A). The other three operons (Fig. 2C) that have YtrA binding peaks were not identified in

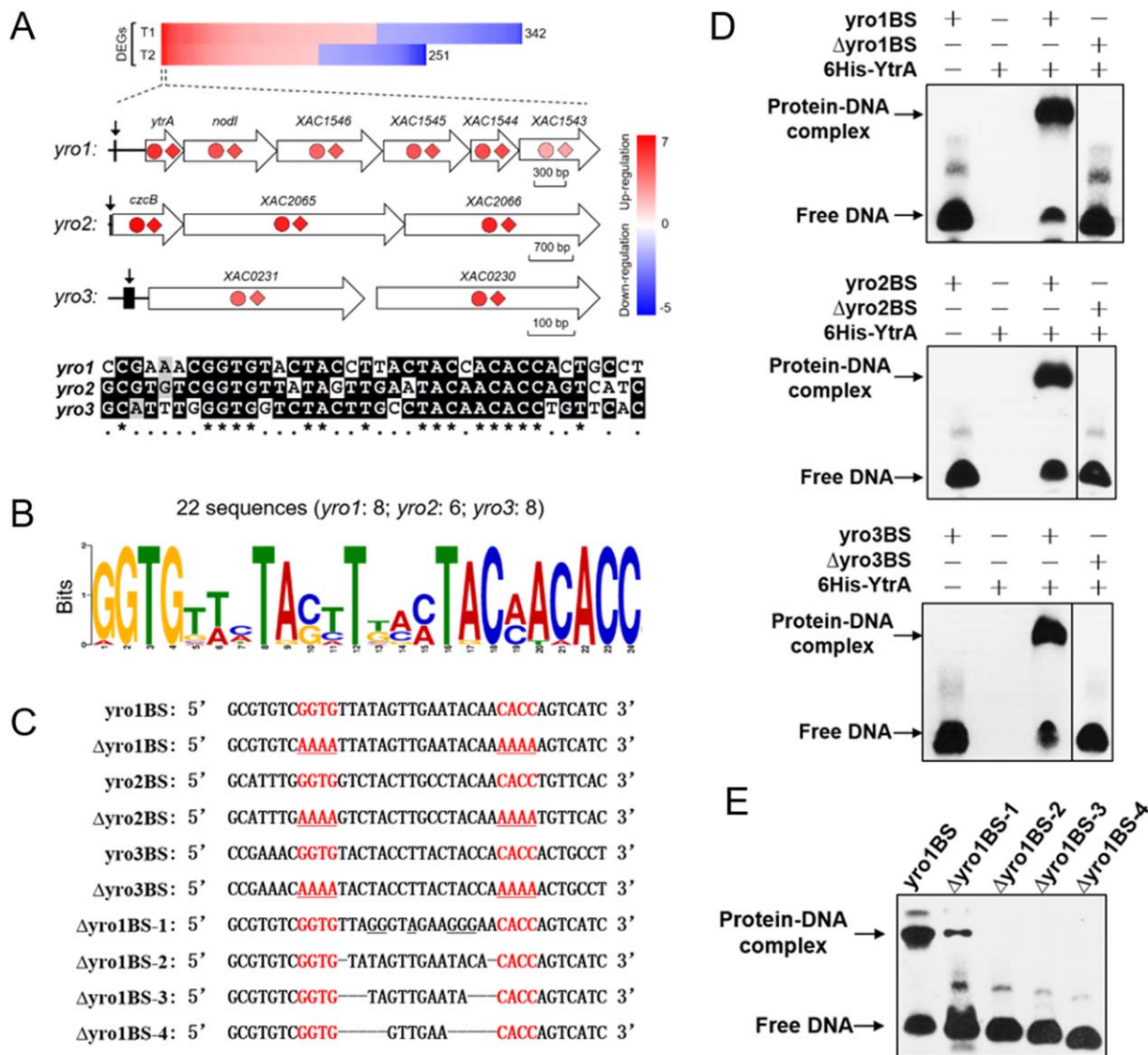


**Fig. 3** YtrA regulates *yro1*, *yro2* and *yro3* regulons and binds to the GGTG-N<sub>16</sub>-CACC palindromic motif. (A) Combined chromatin immunoprecipitation-exonuclease (ChIP-exo) and microarray data analysis revealed three operons directly regulated by YtrA. The genes identified by ChIP-exo were present in the top 30 differentially expressed genes (DEGs) of the microarray data at both T1 and T2 time points. Red represents up-regulation and blue represents down-regulation. The fold changes of genes in the three operons at T1 and T2 are illustrated by coloured circles and diamonds, respectively. The YtrA binding positions are marked with arrows. Sequence alignment of YtrA binding sites is shown below the schematic graph. A 38-bp sequence between two peaks generated by ChIP-exo was extracted from each regulon. Conserved nucleotides are marked with asterisks. (B) Sequence logo representation of the YtrA binding motif. In total, 22 sequences were submitted to MEME for motif identification. Sequences are listed in Table S2. (C) Sequences of probes used in electrophoretic mobility shift assay (EMSA). Underlined nucleotides indicate the mutations. (D) YtrA binds to motifs located at promoter regions of *yro1*, *yro2* and *yro3*, respectively. EMSA experiments were conducted in the presence of purified 6His-YtrA and the corresponding probes listed in (C). (E) Influences of mutated nucleotides on YtrA-DNA interaction. The sequences of the indicated probes are listed in (C). Straight lines indicate deletion of the corresponding nucleotides.



the microarray results and were excluded from further analysis. A conserved palindromic motif GGTG-N<sub>16</sub>-CACC was identified in the three YtrA binding sequences (Fig. 3B) and other *Xanthomonas* spp. (Table S2, see Supporting Information). The putative YtrA binding motif was also identified in *Stenotrophomonas maltophilia*, *Pseudoxanthomonas suwonensis* and *Fraxetria aurantia* based on the phylogenetic tree (Fig. S2, Table S2, see Supporting Information).

To verify whether YtrA binds to the GGTG-N<sub>16</sub>-CACC motif *in vitro*, purified 6His-YtrA and 38-bp double-stranded oligonucleotide probes containing the YtrA binding motif corresponding to *yro1*, *yro2* and *yro3* promoter regions (Fig. 3C) were used to ascertain DNA–protein interaction by EMSA. Motility shift was observed for the DNA probes with addition of the purified 6His-YtrA (Fig. 3D). Mutation of the motif GGTG-N<sub>16</sub>-CACC to AAAA-N<sub>16</sub>-AAAA abolished the motility shift (Fig. 3C,D), suggesting that the palindromic motif GGTG-N<sub>16</sub>-CACC is critical for YtrA binding (Fig. 3C,D). In addition, 'GGTG' and 'CACC', 'TA', 'T' and 'TAC' were also conserved within the 16 nucleotides between the palindromic sequences. Mutation of these conserved nucleotides significantly decreased protein–probe binding (Fig. 3E), indicating that these nucleotides are required for efficient binding of YtrA to its motif. We also tested whether the length of nucleotides between the palindromic sequences contributes to DNA–protein binding. A series deletion of nucleotides abolished YtrA binding to the probe (Fig. 3E). Taken together, these results suggest that YtrA specifically binds to a palindromic motif GGTG-N<sub>16</sub>-CACC in the promoters of target genes. The intermediate sequence also plays an important role in DNA–protein interaction.

### YtrA plays multiple roles in cellular processes

Based on the annotation from the J. Craig Venter Institute (JCVI) role categories, 424 differentially expressed genes (DEGs) identified by microarray were classified into 16 functional groups (Fig. S3, see Supporting Information). Analysis of the microarray data revealed that YtrA was involved in the regulation of multiple cellular processes, including motility and adhesion, oxidative stress, extracellular enzyme production and iron uptake (Table 1).

To test whether mutation of *ytrA* affects bacterial motility and adhesion, bacterial swimming and biofilm formation were tested. The swimming motility of the *ytrA* mutant was significantly reduced compared with the wild-type. The motility deficiency of the mutant was restored to the wild-type level by expression of YtrA in the mutant (Fig. S4A, see Supporting Information). Compared with the wild-type and complementation strain, the *ytrA* mutant formed a reduced biofilm in a glass tube (Fig. S4B).

The expression of *katE*, a monofunctional catalase which contributes to the virulence of *Xac* (Tondo *et al.*, 2010), was down-regulated in the *ytrA* mutant. The catalase activity of the *ytrA* mutant was significantly lower than that of the wild-type and complementation strains (Fig. S5A, see Supporting Information).

In addition, the resistance of *Xac* to hydrogen peroxide (H<sub>2</sub>O<sub>2</sub>) was significantly affected by the mutation of *ytrA* (Fig. S5B). The living cell population of the *ytrA* mutant was reduced more than 1000 times by incubation for 30 min with H<sub>2</sub>O<sub>2</sub>. However, less than a 10-fold population reduction was observed for the wild-type and complementation strains (Fig. S5B).

Extracellular enzymes, e.g. pectate lyase and  $\alpha$ -amylase, are involved in the development of canker symptoms and multiplication of *Xac* in citrus (Lin *et al.*, 2010, Yamazaki *et al.*, 2008). The mutation of *ytrA* significantly down-regulated the expression of *amy*, *egl* and *engXCA*, which encode an  $\alpha$ -amylase and cellulases, respectively (Table 1). Consistently, the *ytrA* mutant was deficient in the production of amylase and cellulose, whereas the complementation strain produced similar amylase and cellulose to the wild-type (Fig. S6A,B, see Supporting Information).

Iron is an essential nutrient for bacterial growth and plays an important role in the virulence of pathogenic bacteria (Litwin and Calderwood, 1993). Mutation of *ytrA* resulted in the over-expression of *lysA*, *iucA*, *yceE*, *XAC3177* and *XAC3178*, which are located in a *Xanthomonas* siderophore synthesis (*xss*) gene cluster in *X. oryzae* pv. *oryzae* (Pandey and Sonti, 2010). In addition, the expression of multiple genes encoding iron siderophore receptors, e.g. *pfeA*, *fhuA*, *fvpA*, *fecA*, *fhuE* and *phuR*, was significantly up-regulated in the *ytrA* mutant (Table 1). To test whether YtrA regulates siderophore production, the bacterial strains were examined on chrome-azuroil S-agar (CAS) medium. The *ytrA* mutant produced a larger halo zone than the wild-type and complementation strains on the plate (Fig. S7A, see Supporting Information), which typically indicates an overproduction of siderophore (Schwyn and Neilands, 1987). Moreover, a significant reduction in growth rate of the *ytrA* mutant compared with the wild type and complementation strains was observed in PS medium (see Experimental procedures) with the addition of the ferrous iron chelator 2,2'-dipyridyl (DP) at final concentrations of 100 and 150  $\mu$ M (Fig. S7B).

### YtrA regulates the expression of T3SS and type III effectors (T3Es)

Microarray data showed that YtrA regulates T3SS and T3Es, which are determinants of bacterial pathogenicity. All of the 25 *hrp* genes, two key regulators *hrpG* and *hrpX*, and 13 T3E genes were up-regulated in the *ytrA* mutant (Table 1). As the up-regulated T3SS and T3Es in XVM2 could not explain the impaired virulence of the *ytrA* mutant, expression of *hrp* genes *in planta* was monitored using QRT-PCR. YtrA positively regulated the expression of *hrpX*, *hrpG*, *hrpB1*, *hrcU* and *hrcQ* at 48 and 72 h post-inoculation (hpi) in the host plant (Fig. 4A).

In the light of the down-regulation of T3SS in the *ytrA* mutant in the citrus plant, we investigated whether the virulence deficiency in the *ytrA* mutant could be restored by constitutive expression of *hrpG* or *hrpX*, as HrpG and HrpX are key virulence

**Table 1** Selected genes regulated by YtrA.\*

Functional groups <sup>†</sup>	Gene or ID locus <sup>‡</sup>	log <sub>2</sub> FC, M/W <sup>§</sup>
Regulatory functions		
Two-component system	<i>XAC1228, XAC1229</i>	3.6–4.4
Sigma factor	<i>fliA, rpoN</i>	–1.7 to –2.7
Sigma factor	<i>prtI</i>	2.1
Other	<i>XAC0807, pcaQ, XAC1548, salR</i>	1.8–6.1
Other	<i>phoU, XAC2166</i>	–1.6 to –2.4
Cellular process		
Chemotaxis and motility	<i>flgBCDEFGHIJKL, fliEFGHILMNOPQR, fliC, flhF, fleN, tsr<sub>XAC1893</sub>, tsr<sub>XAC1894</sub>, tsr<sub>XAC1895</sub>, tsr<sub>XAC1897</sub>, tsr<sub>XAC1899</sub>, tsr<sub>XAC1900</sub>, cheA<sub>XAC1903</sub>, cheA<sub>XAC1930</sub>, cheA<sub>XAC2865</sub>, cheW<sub>XAC1906</sub>, cheW<sub>XAC2867</sub>, cheY<sub>XAC1904</sub>, cheY<sub>XAC1932</sub>, cheRVZ, motBC, mcp<sub>XAC1996</sub>, mcp<sub>XAC2448</sub>, mcp<sub>XAC2866</sub>, mcp<sub>XAC3132</sub></i>	–1.6 to –3.1
Detoxification	<i>katE, btuE, yapH, XAC0540</i>	–1.6 to –3.6
Iron uptake		
Iron binding and transport	<i>pfeA, fhuA<sub>XAC2941</sub>, fpvA, fecA, fhuA<sub>XAC1435</sub>, fhuE<sub>XAC3370</sub>, fhuE<sub>XAC3498</sub>, phuR<sub>XAC2829</sub>, phuR<sub>XAC0823</sub>, feoB, XAC0492</i>	1.9–4.2
Siderophore biosynthesis	<i>lysA, iucA, yceE, XAC3177, XAC3178</i>	1.7–4.1
Iron binding and transport	<i>fhuA<sub>XAC2830</sub>, fyuA, btuB, brf, XAC1149</i>	–1.6 to –2.6
Type III secretion system (T3SS) and T3SS effectors		
T3SS key regulators	<i>hrpG, hrpX</i>	1.7–1.9
T3SS	<i>hrcCJNQRTUV, hrpB1B2B4B5B7D5D6, hpa1, hpa2, hpaABFP, XAC0395</i>	1.6–2.7
T3SS effectors	<i>avrXacE2, avrBs2, hrpW, XAC0277, XAC0754, XAC1208, XAC2009, XAC3085, XAC3090, XAC3230, XAC3666, XAC4213, XAC4333</i>	1.6–2.3
T3SS effectors	<i>XAC1209<sup>¶</sup>, XAC1210<sup>¶</sup></i>	–1.6 to –1.7
Energy metabolism and central intermediary metabolism		
Extracellular enzymes	<i>amy, egl, engXCA</i>	–1.7 to –3.1
The tricarboxylic acid (TCA) cycle	<i>mls, aceA</i>	–3.0 to –5.0
Oxidoreductase	<i>yagRS, petABC, vanB, aslB, XAC3738</i>	–1.6 to –4.0
Oxidase	<i>cox3, cox11, ctaCD</i>	–1.7 to –1.9
Dehydrogenase	<i>yagT, fdh, ybdR, gcd</i>	–1.6 to –4.4
Dehydrogenase	<i>acdA</i>	2.2
DNA metabolism		
DNA recombination, replication and repair	<i>lig3, XAC0035</i>	–2.0 to –2.2
DNA recombination, replication and repair	<i>XAC3006</i>	1.7
Fatty acid and phospholipid metabolism		
Degradation	<i>paaF, fedE9, XAC0375</i>	1.8–2.0
Other	<i>mdbB</i>	1.6
Protein fate		
Folding and stabilization	<i>groESL, htpX, hslVU</i>	1.6–1.8
Secretion and trafficking	<i>tolC</i>	3.8
Modification and repair	<i>pcm</i>	3.1
Degradation	<i>XAC2832, XAC0609, XAC3309, dcp<sub>XAC1456</sub>, dcp<sub>XAC0249</sub>, XAC0262, XAC0591, XAC0628, ptrB, pepN<sub>XAC1159</sub>, pepN<sub>XAC3318</sub>, XAC1204, XAAC2745, XAC2999, sppA, XAC4106</i>	1.6–6.1
Degradation	<i>pfpl, rrpX, XAC0465</i>	–1.7 to –3.3

\*Data were selected from the microarray results. Detailed information is provided in Table S3.

<sup>†</sup>Functional groups were manually modified based on the result of Fig. S3 for the easy understanding of the content.

<sup>‡</sup>Genes annotated with the same name are indicated by their specific ID locus.

<sup>§</sup>FC, fold change; M/W, mutant vs. wild-type.

<sup>¶</sup>Inactive/pseudogene.

regulators responsible for the expression of T3SS. Ectopic expression of *hrpG* fully restored the virulence of the *ytrA* mutant to the wild-type level (Fig. 4B,C). Constitutive expression of *hrpX* partially restored the virulence of the *ytrA* mutant (Fig. 4B,C). Consis-

tently, deficient virulence of the *ytrA* mutant in HR induction was restored by constitutive expression of *hrpG* or *hrpX* (Fig. 1C). Taken together, our results suggest that YtrA transcriptionally regulates T3SS and T3Es. The regulation is probably indirect as the

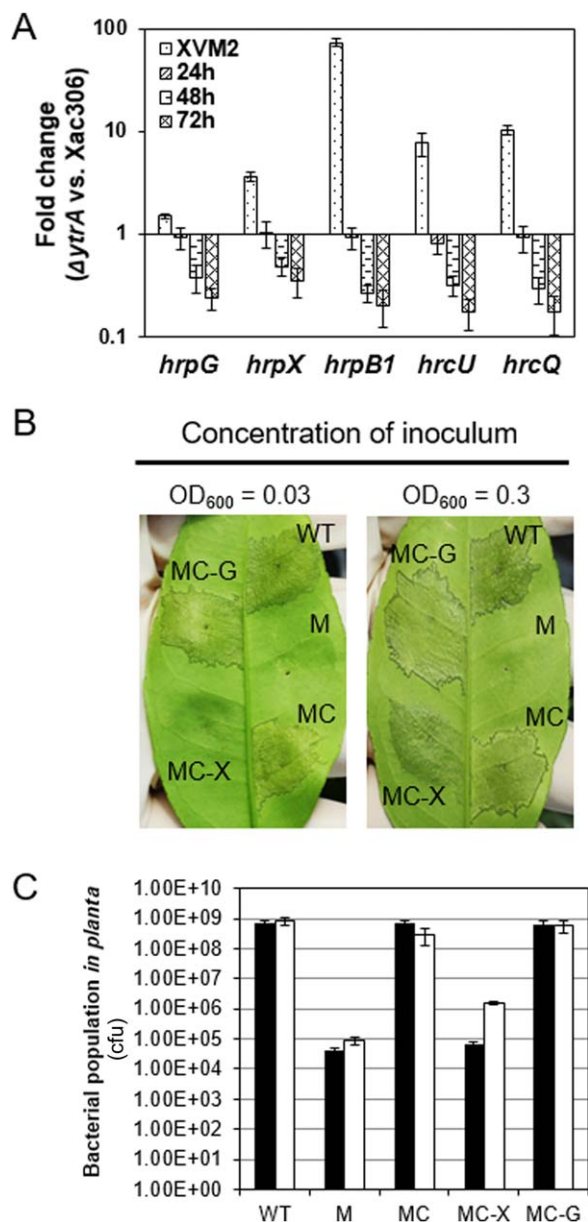


**Fig. 4** YtrA regulates the expression of the bacterial type III secretion system (T3SS) and type III effectors (T3Es). (A) YtrA positively regulates T3SS in *Xanthomonas citri* ssp. *citri* (*Xac*) in planta. The wild-type and mutant were inoculated in Duncan grapefruit. The relative expression (mutant vs. wild-type) of the genes of interest at different time points is shown as relative values on a logarithmic scale. (B) Ectopic expression of *hrpG* and *hrpX* restored the deficient virulence in the *ytrA* mutant. *Xac* strains were inoculated in the host plant grapefruit with starting concentrations of OD<sub>600</sub> = 0.3 or 0.03. Inoculated leaves were photographed at 3 days post-inoculation (dpi). (C) The bacterial population *in planta* was tested at 6 dpi. Black and white columns indicate that strains were inoculated with starting concentrations of OD<sub>600</sub> = 0.03 and 0.3 respectively. WT, *Xac* 306 with empty vector pUFR053; M, *ytrA* mutant with pUFR053; MC, *ytrA* mutant with p53-YtrA; MC-X, *ytrA* mutant with p53-HrpX; MC-G, *ytrA* mutant with p53-HrpG.

YtrA binding motif was not identified in the promoter regions of T3SS and T3E genes (Fig. 2C).

### Critical residues of YtrA required for bacterial virulence

Several conserved residues, including residues at the N-terminal HTH domain, were mutated by site-direct mutagenesis. PIY (11–13), PSVR (36–39), LNPIT (47–51) and RRGLG (68–72) were mutated to AIA, ASAA, ANAIA and ARALA, respectively (Fig. S8A, see Supporting Information). The expression of all mutated proteins was subjected to immunoblot analysis to rule out the influence of mutations on protein stability (Fig. S8C). The *ytrA* mutants expressing different YtrA mutations were inoculated on citrus plants. YtrA mutations failed to restore the virulence of the *ytrA* mutant (Fig. S8B), whereas the wide-type YtrA fully complemented the virulence of the *ytrA* mutant (Fig. 1A), suggesting that these conserved residues are required for YtrA-regulated bacterial virulence.

### YtrA regulatory activity in the host and medium

Previous reports have shown that YtrA in *X. campestris* pv. *campestris* negatively regulates itself in XVM2 medium, but positively regulates itself in the host (An *et al.*, 2011). We tested whether a similar phenomenon also occurs in *Xac*. The expression levels of all tested genes (*XAC1547*, *XAC1546* and *XAC1545* representing the *yro1* operon, *czcB* representing the *yro2* operon, and *XAC0231* and *XAC0230* representing the *yro3* operon) were greater in the *ytrA* mutant than in the wild-type strain in both medium (NB and XVM2 media) and *in planta* (Fig. 5A). To confirm that YtrA is a constant repressor of the aforementioned genes (Fig. 5A) in both medium and host, native and mutant promoters (GGTG to AAAA) (Fig. S9A,B, see Supporting Information) of *yro1*, *yro2* and *yro3* were fused with the  $\beta$ -glucuronidase (GUS) reporter gene. The resulting GUS constructs were introduced into the wild-type and *ytrA* mutant, and GUS activities were assayed. The *lac* promoter was used as a control to ascertain no GUS expression preference between the wild-type and mutant (Fig. 5B). Consistent with our QRT-PCR results, GUS expression driven by the native promoters of the three different YtrA regulons was apparently higher in the *ytrA* mutant than in the wild-type strain according to histochemical staining and quantification of GUS activity (Fig. 5B). GUS activities driven by mutant promoters were higher than those driven by native promoters in the wild-type strain in NB and XVM2 medium and *in planta*, further confirming that YtrA represses the expression of *yro1*, *yro2* and *yro3* (Fig. 5B,C).

### Over-expression of *yro3* operon attenuates *Xac* virulence and T3SS expression

To investigate whether *yro* regulons are involved in the regulation of bacterial virulence, three *yro* regulons were over-expressed in

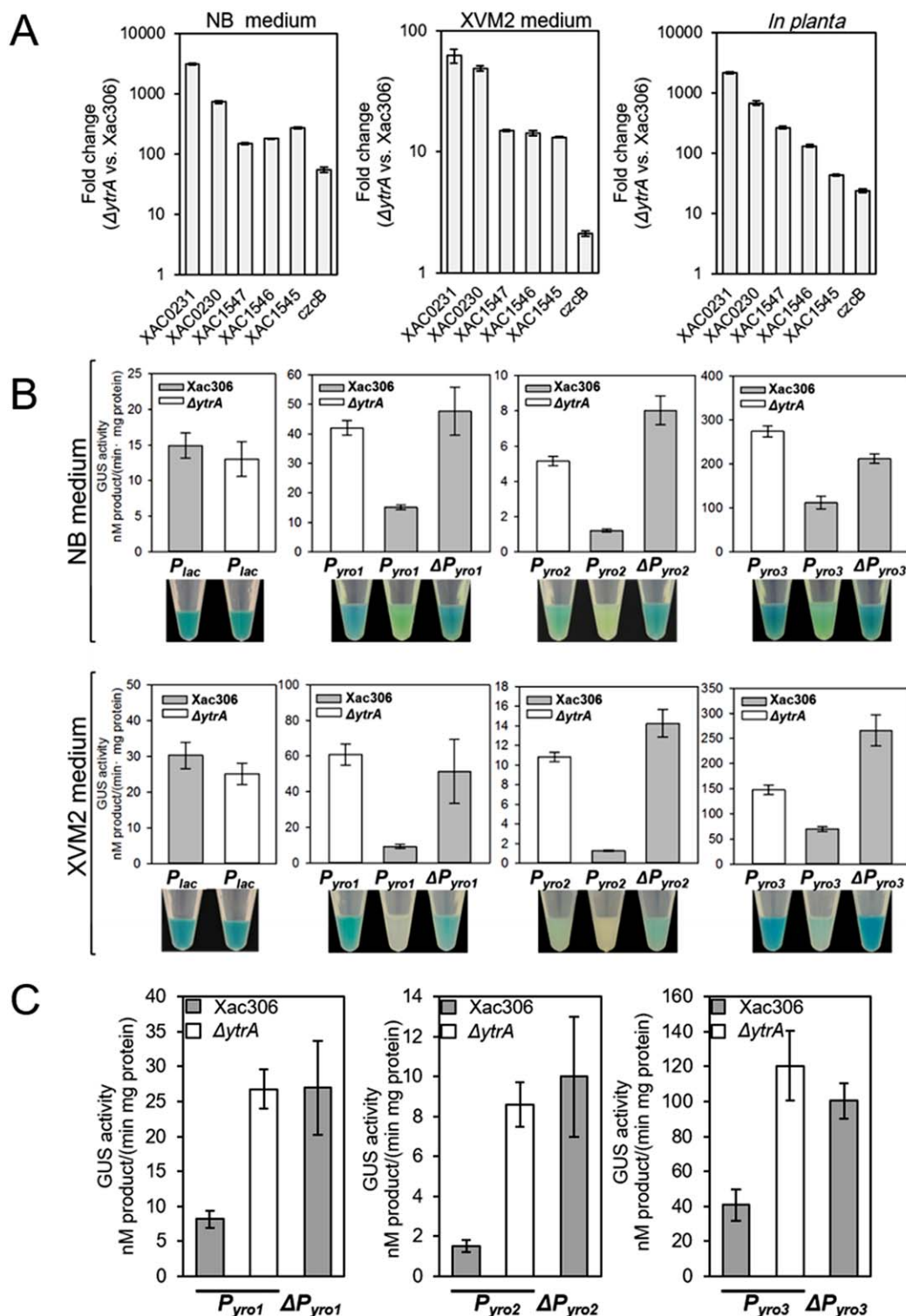


**Fig. 5** YtrA is a transcriptional repressor in medium and host. (A) Relative expression of YtrA-regulated genes in nutrient broth (NB), a plant-mimic medium (XVM2) and *in planta*. Cells were collected from overnight culture or recovered from inoculated leaves at 5 days post-inoculation (dpi). Fold change values are plotted as relative values on a logarithmic scale. (B) Quantification of  $\beta$ -glucuronidase (GUS) activity and histochemical staining of GUS expression in *Xanthomonas citri* ssp. *citri* (Xac) cells grown in NB and XVM2 medium. Promoter length and sequences are shown in Fig. S9. Four replicates were performed and one tube is presented. (C) Quantification of GUS activity of Xac cells grown *in planta*.



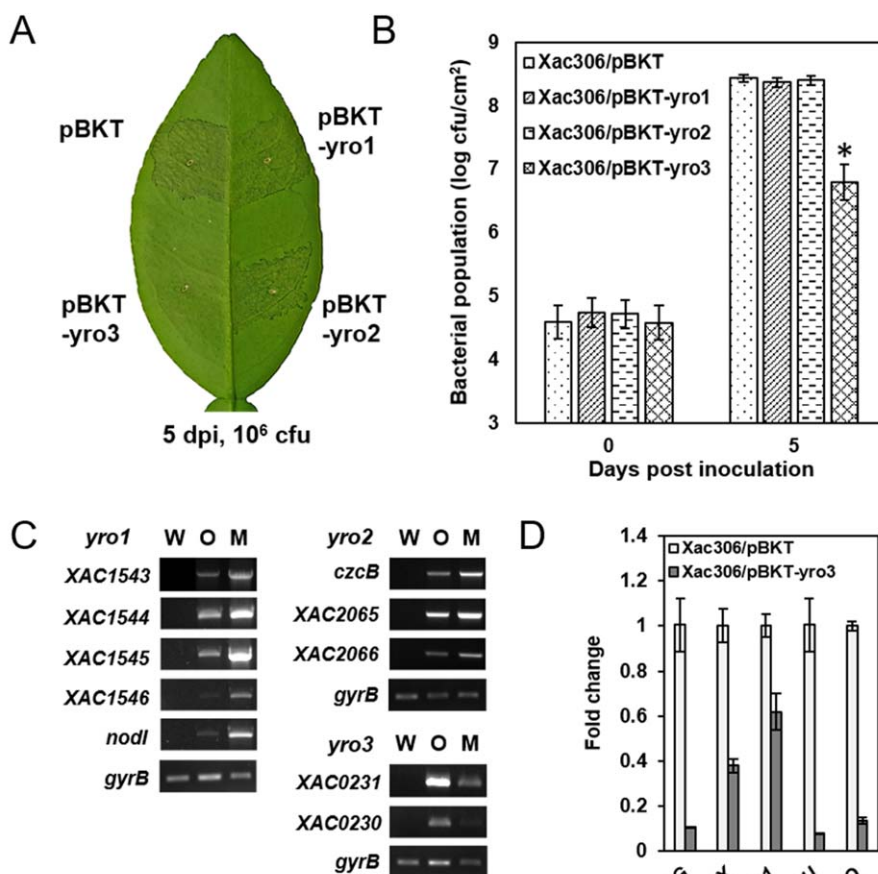


**Fig. 6** Over-expression of the *yro3* operon attenuates bacterial virulence. (A) Bacterial pathogenicity on citrus plant. *Xanthomonas citri* ssp. *citri* (*Xac*) wild-type strains containing pBKT, pBKT-*yro1*, pBKT-*yro2* and pBKT-*yro3* were infiltrated into citrus leaves at an initial concentration of  $10^6$  colony-forming units (cfu/mL). Leaves were photographed at 5 days post-inoculation (dpi). (B) Bacterial population *in planta*. Bacterial cells were recovered from the inoculated leaves at 0 and 5 dpi, and the values are the means from three repeats. Means  $\pm$  standard deviations are plotted. Asterisks indicate a statistically significant difference (Student's *t*-test,  $P < 0.01$  versus the wild-type). (C) Verification of gene expression using semi-quantitative reverse transcription-polymerase chain reaction (QRT-PCR). (D) Relative gene expression determined by QRT-PCR. Fold change values are shown and normalized using the expression of *gyrB*.

the wild-type strain under the control of the *trp* promoter. The over-expression constructs were introduced into the wild-type strain for pathogenicity assay *in planta*. Empty vector was used as a negative control. The expression of individual genes from all three different operons was confirmed by QRT-PCR (Fig. 6C). Intriguingly, over-expression of *yro3* attenuated *Xac* virulence, whereas over-expression of *yro1* and *yro2* did not (Fig. 6A). The growth of the *yro3*-expressing strain was significantly ( $P < 0.01$ ) slower than that of strains expressing *yro1*, *yro2* and empty vector (Fig. 6B). To test whether an individual protein located in the *yro3* operon was a crucial factor in the decrease in bacterial virulence, *XAC0231* and *XAC0230* were over-expressed in the wild-type and protein expression was confirmed by immunoblot (Fig. S10B, see Supporting Information). Cells expressing *XAC0231* or *XAC0230* showed similar canker symptoms to cells harbouring empty vector (Fig. S10A). To rule out the possibility of delayed bacterial growth caused by over-expression of *yro* operons, we assessed the growth rates of strains over-expressing *yro1*, *yro2* and *yro3* in NB and XVM2 medium. Over-expression of the three operons did not affect bacterial growth (Fig. S11A,B, see Supporting Information). Expression of T3SS was down-regulated by QRT-PCR in the *yro3* over-expressing strain when cells were grown *in planta* (Fig. 6D). Taken together,

our results indicate that *XAC0231* and *XAC0230* play a role in the negative regulation of T3SS and bacterial virulence.

## DISCUSSION

In this study, we have identified the direct targets of YtrA in *Xac* using both microarray and ChIP-exo analyses. Microarray assay identified a total of 424 genes regulated by YtrA (Fig. 2A), whereas ChIP-exo identified a total of six direct targets (Fig. 2C). Although microarray analysis provides a comprehensive view of the genome-wide gene expression profile of YtrA, it could not distinguish between direct targets and indirectly regulated genes. ChIP-exo delivers near single-nucleotide resolution to target identification and decreases the background noise by digesting contaminating DNA; therefore, it has become a widely applied tool in the identification of DNA binding sites and targets of regulators (Mahony and Pugh, 2015; Rhee and Pugh, 2011). Among the six direct targets of YtrA identified by ChIP-exo, only three (*yro1*, *yro2* and *yro3*) were identified by microarray analysis. The palindromic GGTG-N<sub>16</sub>-CACC binding motif of YtrA was identified and confirmed in the promoter regions of *yro1*, *yro2* and *yro3* (Fig. 3B,D), but not in the other three genes (Fig. 2C), which further indicates

that *yro1*, *yro2* and *yro3* are the direct targets of YtrA. We reasoned that the other three genes identified in ChIP-exo (Fig. 2C) might result from non-specific interaction in ChIP as they are not identified in the microarray data.

We further defined and experimentally validated the YtrA binding motif, the palindromic GGTG-N<sub>16</sub>-CACCC motif (Fig. 3A–D), compared with previous predictions (Rigali *et al.*, 2002; Suvorova *et al.*, 2015). We found the *yro2* operon to be a new YtrA direct target that has not been predicted previously. The *yro2* operon consists of *czcB*, *XAC2065* and *XAC2066*, which might encode a putative cation efflux system involved in resistance to multiple heavy metals, e.g. cadmium, cobalt, zinc, nickel, chromate, and to antimicrobial agents (Nies, 2003; Stahler *et al.*, 2006; Venter *et al.*, 2015; Vila *et al.*, 2007). Interestingly, the palindromic GGTG-N<sub>16</sub>-CACCC motif was not only identified in *Xanthomonas*, but also in many other bacteria, e.g. *S. maltophilia*, *P. suwonensis* and *F. aurantia*, whose YtrA shares 92%, 89% and 68% identity with YtrA<sub>Xac</sub>, respectively (Fig. S2, Table S2). Taken together, these data suggest that YtrA binding to the palindromic motif GGTG-N<sub>16</sub>-CACCC is a widespread phenomenon.

Multiple factors contribute to the virulence deficiency of the *ytrA* mutant. First, expression of *katE*, a monofunctional catalase, was down-regulated in the *ytrA* mutant (Fig. S5A). KatE is critical for *Xac* to resist H<sub>2</sub>O<sub>2</sub>, a reactive oxygen species (ROS) (Tondo *et al.*, 2010). Consistently, resistance of *Xac* to H<sub>2</sub>O<sub>2</sub> was significantly affected by the mutation of *ytrA* (Fig. S5B). *Xac* needs to overcome ROS, which plants employ to defend against invading phytopathogens (Hammond-Kosack and Jones, 1996). The reduced tolerance of the *ytrA* mutant to ROS probably contributes to its reduced growth *in planta* (Fig. 1B). Second, the reduced expression of the genes responsible for extracellular enzymes, e.g. pectate lyase and  $\alpha$ -amylase (Table 1), and the corresponding decrease in enzyme production (Fig. S6A,B), also contribute to the reduced virulence of the *ytrA* mutant. Pectate lyase and  $\alpha$ -amylase are involved in the development of canker symptoms and the multiplication of *Xac* in citrus (Lin *et al.*, 2010; Yamazaki *et al.*, 2008). Lastly, YtrA positively regulates the expression of T3SS genes, e.g. *hrpX*, *hrpG*, *hrpB1*, *hrcU* and *hrcQ*, in the host plant (Fig. 4A). Over-expression of the T3SS regulator HrpX failed to fully restore virulence in the *ytrA* mutant, which further confirms that the decreased virulence in the *ytrA* mutant is not only caused by a down-regulated T3SS.

One puzzle was observed for the YtrA regulation of T3SS genes *in planta* and *in vitro*. YtrA represses T3SS genes *in vitro*, but positively regulates T3SS genes *in planta*. As the YtrA binding motif was not identified in the promoters of T3SS genes (Fig. 2C), we reasoned that YtrA regulation of T3SS genes is via an indirect mechanism. An elegant hypothesis has been proposed to address a similar phenomenon in *X. campestris* pv. *campestris* (An *et al.*, 2011). In their hypothesis, An *et al.* (2011) proposed that a plant signal molecule induces the expression of an unknown regulator

which suppresses *hpaR1* expression. However, this suppression can be inactivated by HapR1, so that the *hpaR1* gene can be expressed in the wild-type cells, but not in the *hpaR1*-deficient mutant cells. In medium, *hpaR1* can be expressed without HapR1 because of the lack of the specific plant signal molecule. It remains to determine whether a similar mechanism exists in *Xac*.

Interestingly, the over-expression of the *yro3* operon attenuates *Xac* virulence and T3SS expression. The *yro3* operon contains two open reading frames (ORFs): *XAC0230* and *XAC0231*. *XAC0230* encodes TrmL, a tRNA modification enzyme catalysing the methyl transfer from S-adenosyl-L-methionine to the 2'-OH of the ribose at the nucleotide 34 wobble position of two isoacceptors tRNA<sup>Leu</sup><sub>CmAA</sub> and tRNA<sup>Leu</sup><sub>cmm5UmAA</sub> (Benitez-Paez *et al.*, 2010). Notably, the crystal structure revealed that TrmL forms a homodimer and can independently catalyse methyl transfer through the conserved C-terminal half of the SPOUT domain for catalysis and less conserved N-terminal domain for tRNA recognition (Liu *et al.*, 2013). *XAC0231* encodes a hypothetical protein without a known function. A signal peptide is predicted for *XAC0231* by SignalP 4.1 at the N-terminal 26 residues, suggesting that *XAC0231* is likely to be secreted into the bacterial periplasm. Our results showed that the over-expression of the *yro3* operon attenuated *Xac* virulence, whereas individual expression of TrmL or *XAC0231* did not affect pathogenicity (Fig. S10). Therefore, although tRNA modification has been reported to be implicated in bacterial virulence in several plant and animal pathogens (Cho and Caparon, 2008; Durand *et al.*, 2000; Kinscherf and Willis, 2002; Shippy and Fadl, 2015; Shippy *et al.*, 2013), the mechanism of *Xac* virulence regulation mediated by the *yro3* operon remains unknown.

In conclusion, we experimentally identified YtrA direct targets and comprehensively analysed YtrA-associated phenotypes in *Xac*. Combining microarray and ChIP-exo data, we revealed that YtrA, as a transcriptional repressor in NB, XVM2 medium and host, binds to a palindromic motif GGTG-N<sub>16</sub>-CACCC located at the promoter regions of the *yro1*, *yro2* and *yro3* operons. YtrA also plays a pivotal role in bacterial virulence and HR induction. Considering the critical role of YtrA in bacterial pathogenicity, we can design novel disease control approaches by the identification of compounds targeting YtrA. In addition, we experimentally confirmed that the abolished virulence of the *ytrA* mutant is caused by the over-expression of the *yro3* operon via an unknown mechanism. Studies are needed to further elucidate the role of the *yro3* operon in bacterial virulence.

## EXPERIMENTAL PROCEDURES

### Bacterial strains, grown conditions, plasmids and primers

The bacterial strains and plasmids used in this work are listed in Table S3 (see Supporting Information). Primers are listed in Table S4 (see Supporting

Information). The *Escherichia coli* strain was cultured at 37 °C in Luria–Bertani (LB) medium. *Xac* strains were cultured at 28 °C on nutrient agar (NA) plates, in nutrient broth (NB) or XVM2 medium. Plasmids in this work were constructed in JM109 cells. BL21(DE3) was used for YtrA purification. The *ytrA* EZ-Tn5 mutant was used in microarray analysis and the deletion mutant was used for ChIP-exo. When required, growth media were supplemented with ampicillin (50 µg/mL), gentamycin (5 µg/mL), kanamycin (50 µg/mL), rifamycin (50 µg/mL) and spectinomycin (100 µg/mL).

### ChIP-exo

ChIP-exo experiments were carried out by Peconic LLC (State College, PA, USA) essentially as described previously (Reja *et al.*, 2015). The procedure consists of an immunoprecipitation step with magnetic beads, followed by DNA polishing, a step of Illumina adaptor ligation (ExA2) and a digestion by lambda and RecJ exonuclease on the beads. A primer was then annealed to the EXA2 adaptor and extension was performed using  $\Phi$ 29 DNA polymerase. Products were A-tailed and ligated with a second Illumina adaptor for PCR amplification and gel purification. Sequencing was performed using an Illumina HiSeq 2000, San Diego, CA, USA. Uniquely aligned sequence tags were mapped to the *Xac* 306 genome using BWA (version 0.5.9-r16) (Li and Durbin, 2009).

### RNA extraction and microarray assay

A single colony of wild-type and mutant was inoculated in XVM2 broth and incubated at 28 °C and 200 rpm overnight. Cells were re-inoculated into fresh XVM2 broth with a starting concentration of  $OD_{600} = 0.03$  and incubated at 28 °C and 200 rpm. Bacterial cells were collected at two time points in the exponential growth stage and were treated immediately with two volumes of RNA protect bacterial reagent (Qiagen, Valencia, CA, USA). RNA was extracted using an RNeasy mini kit (Qiagen). Contaminated genomic DNA was removed by a TURBO DNA-free kit (Ambion, Austin, TX, USA). The RNA quality was assessed using an Agilent 2100 bioanalyser (Agilent Technologies, Palo Alto, CA, USA).

The 8-by-15-K DNA *Xac* oligonucleotide microarray chip covering the whole genome of strain 306 was used in this study. The microarray experiment was conducted at the Interdisciplinary Center for Biotechnology Research Microarray Core Facility, University of Florida, FL, USA. The extracted RNA (5 µg) was used to generate cDNA and then labelled with either cy3 or cy5 using a Fairplay III microarray labelling kit (Agilent Technologies). A total of 300 ng of labelled cDNA per sample was used for hybridization employing a Gene Expression Hybridization Kit (Agilent Technologies). Four independent biological replicates were performed for two time point comparisons with dye-swap design. The arrays were scanned using a dual-laser DNA microarray scanner (Model G2505C; Agilent Technologies). The data were extracted from a scanned image using Feature Extraction 10.1.1.1 software (Agilent Technologies).

The microarray data were analysed as described previously (Guo *et al.*, 2011). Briefly, the raw data were imported into the R environment and statistical tests were performed using BioConductor statistical software (Gentleman *et al.*, 2004).  $\log_2$ -transformed fold change values were used for statistical analysis. The *P* values were adjusted using the Benjamini–Hochberg method, designated as FDR (Benjamini and Hochberg, 1995). DEGs were ranked based on FDR and  $\log_2$  fold change. Genes with

FDR < 0.05 and a minimum absolute value of  $\log_2$  fold change > 1.585 (equivalent to three-fold) were considered to be significant DEGs.

### Stress resistance assay

The resistance assay against  $H_2O_2$  was performed as reported previously (Yan *et al.*, 2012) with modifications. Wild-type, mutant and complemented strains were cultured to stationary phase (24 hpi) in XVM2 broth in a 28 °C growth shaker. The bacterial population was adjusted to  $OD_{600} = 0.3$ .  $H_2O_2$  was added to the bacterial suspension with a final concentration of 20 mM. The challenged bacterial cells were sampled at different time points and the living cell population was determined by serial dilution on an XVM2 plate.

To test the bacterial survival under iron-limited conditions, the *Xac* strains were cultured in PS medium (for 1 L broth: 10 g peptone, 10 g sucrose and 1 g sodium glutamate) with a starting concentration of  $OD_{600} = 0.03$ . For iron-limited growth conditions, DP (a specific  $Fe^{2+}$  chelator) was added with final concentrations of 50, 100, 150 and 200 µM. The bacterial cultures were incubated at 28 °C with shaking at 200 rpm. The growth of each strain was determined at 24 hpi by checking the  $OD_{600}$  value.

### Cell extract preparation and catalase activity assay

The catalase activity assay was performed as described previously (Yan and Wang, 2011) with modifications. Briefly, *Xac* strains were cultured to stationary phase (24 hpi) in XVM2 broth. Cells were washed twice and re-suspended in ice-cold 50 mM potassium phosphate buffer (pH = 7.0) and then sonicated for 3 min with a sonicator (Misonix, Sonicator 3000 Newtown, CT, USA). The bacterial lysate was clarified by centrifugation at 13 000 g for 20 min at 4 °C. The protein concentration was determined using a BCA protein assay kit (Novagen, San Diego, CA, USA). Catalase activity was measured spectrophotometrically by following the rate of decrease in absorbance at 240 nm caused by the decomposition of  $H_2O_2$  (Beers and Sizer, 1952). The reaction was performed in 50 mM potassium phosphate buffer (pH = 7.0) containing 50 mM  $H_2O_2$  at room temperature. The absorption coefficient at 240 nm for  $H_2O_2$  was taken to be  $43.6 \text{ m}^{-1} \text{ cm}^{-1}$  (Hildebrandt and Roots, 1975) to calculate the specific activity. One unit of catalase activity was defined as the amount of protein required to decompose 1 µmol  $H_2O_2$ /min under the assay conditions.

### Extracellular enzymes activity and production of siderophore

Extracellular amylase and cellulase activity assays were performed as described previously with modifications (Andro *et al.*, 1984; Yan and Wang, 2012). Bacterial cells were collected from the overnight cultures and re-suspended in fresh XVM2 broth to give a final concentration of  $OD_{600} = 0.3$ . For extracellular amylase activity assay, 2 µL of the cell suspension were inoculated onto an XVM2 plate containing 1% (w/v) starch (Acros Organics, Fair Lawn, NJ, USA), and the plate was incubated at 28 °C for 3 days. The plate was stained using Gram's iodine solution. A transparent halo surrounding the colony against the blue background of the plate indicated the secretion of extracellular amylase. For extracellular cellulase activity assay, 2 µL of the cell suspension were inoculated onto an XVM2 plate containing 0.5% (w/v) carboxymethyl cellulose sodium

salt (Santa Cruz Biotechnology, Santa Cruz, CA, USA), and the plate was incubated at 28 °C for 3 days. The plate was stained using 0.1% Congo Red. A transparent halo surrounding the colony against the red background of the plate indicated the secretion of extracellular cellulase. All assays were repeated three times with three replicates. Only one of the results was presented. To test the production of siderophore, 2 µL of the cell suspension were spot inoculated onto CAS medium (Schwyn and Neillands, 1987), and the plates were incubated for 6 days at 28 °C. The development of an orange halo around the bacterial colony indicated siderophore production. All experiments were repeated more than twice with three replicates each time.

### QRT-PCR

The gene-specific primers used in QRT-PCR are listed in Table S4. To assay bacterial gene expression *in planta*, cells were infiltrated into citrus leaves with an initial OD<sub>600</sub> value of 0.6 and leaves were sampled at the corresponding time points. Total RNA was extracted directly from inoculated leaves. The RNA obtained was subjected to a one-step QRT-PCR assay with a 7500 fast real-time PCR system (Applied Biosystems, Foster City, CA, USA) using a QuantiTect SYBR green RT-PCR kit (Qiagen). The *gyrB* gene was used as an endogenous control. The relative fold change in target gene expression was calculated using the 2<sup>-ΔΔCT</sup> method (Livak and Schmittgen, 2001).

### Plant inoculation and bacterial population

Pathogenicity assay on citrus and the measurement of the bacterial population were performed as described previously (Zhou *et al.*, 2015). The induction of HR by *Xac* cells was performed on *Nicotiana benthamiana* as described previously (Zhou *et al.*, 2015).

### Electrophoretic mobility shift assay (EMSA)

The *ytrA* gene was cloned into pET-28a. Protein was induced and purified according to the manufacturer's instructions (Ni-NTA Agarose Kit, Qiagen). Probe oligonucleotides were synthesized by IDT, Inc (Coralville, IA, USA). DNA labelling was performed using a Pierce™ Biotin 3' End DNA Labelling Kit (Thermo Fisher). EMSA was conducted using a LightShift™ Chemiluminescent EMSA Kit (Thermo Fisher, Waltham, MA, USA).

### GUS assay

For the histochemical staining of *Xac* cells with 5-bromo-4-chloro-3-indolyl-β-D-glucuronide cyclohexylammonium salt (X-Gluc), stationary cell cultures were adjusted to an OD<sub>600</sub> of 1. Then, 1 mL of adjusted culture was pelleted and re-suspended in staining solution containing phosphate-buffered saline (PBS) with 10 mM ethylenediaminetetraacetic acid (EDTA), 0.1% Triton X-100 and 2 mM X-Gluc. Samples were incubated at 37 °C and photographed at specific time points. For measurement of GUS activity, 10 mL of cell cultures with OD<sub>600</sub> = 1 were harvested and re-suspended in PBS buffer in the presence of protease inhibitor cocktail Sigma-Aldrich (St. Louis, MO, USA). Cells were lysed using sonication, and the cleared bacterial lysate was assayed for GUS activity. The total protein amount was determined using a Bio-Rad protein assay kit (Bio-Rad Laboratories, Hercules, CA, USA). A 1.5-mL tube containing 800 µL of GUS assay buffer

[50 mM PBS buffer, pH 7.0, 1 mM EDTA, 5 mM dithiothreitol (DTT), 1.25 mM *p*-nitrophenyl-β-D-glucuronide] and 200 µL of cell lysate was incubated at 37 °C. At the specific time points, a 25-µL reaction aliquot was removed from each sample into a 96-well plate containing 175 µL of stop solution (0.4 M Na<sub>2</sub>CO<sub>3</sub>). The absorbance was measured at 405 nm for each sample against a stopped blank reaction. The linear graph of OD<sub>405</sub> (*y*-axis) vs. time (*x*-axis) was plotted and the slope *S* was characterized. The rate of reaction *R* (nM product/min/mg total protein) was calculated using the equation:  $R = S / (0.02 \times 0.005 \times \text{protein concentration})$ .

### ACKNOWLEDGEMENTS

This study was partially supported by grants from the Florida Citrus Research and Development Foundation and the US Department of Agriculture-National Institute of Food and Agriculture (USDA-NIFA).

### REFERENCES

- Alfano, J.R. and Collmer, A. (2004) Type III secretion system effector proteins: double agents in bacterial disease and plant defense. *Annu. Rev. Phytopathol.* **42**, 385–414.
- An, S.Q., Lu, G.T., Su, H.Z., Li, R.F., He, Y.Q., Jiang, B.L., Tang, D.J. and Tang, J.L. (2011) Systematic mutagenesis of all predicted GntR genes in *Xanthomonas campestris* pv. *campestris* reveals a GntR family transcriptional regulator controlling hypersensitive response and virulence. *Mol. Plant-Microbe Interact.* **24**, 1027–1039.
- Andro, T., Chambost, J.P., Kotoujansky, A., Cattaneo, J., Bertheau, Y., Barras, F., Van Gijsegem, F. and Coleno, A. (1984) Mutants of *Erwinia chrysanthemi* defective in secretion of pectinase and cellulase. *J. Bacteriol.* **160**, 1199–1203.
- Baptista, J.C., Machado, M.A., Homem, R.A., Torres, P.S., Vojnov, A.A. and do Amaral, A.M. (2010) Mutation in the *xpsD* gene of *Xanthomonas axonopodis* pv. *citri* affects cellulose degradation and virulence. *Genet. Mol. Biol.* **33**, 146–153.
- Beers, R. and Sizer, I. (1952) A spectrophotometric method for measuring the breakdown of hydrogen peroxide by catalase. *J. Biol. Chem.* **195**, 133–140.
- Benitez-Paez, A., Villarroya, M., Douthwaite, S., Gabaldon, T. and Armengod, M.E. (2010) YibK is the 2'-O-methyltransferase TrmL that modifies the wobble nucleotide in *Escherichia coli* tRNA(Leu) isoacceptors. *RNA*, **16**, 2131–2143.
- Benjamini, Y. and Hochberg, Y. (1995) Controlling the false discovery rate: a practical and powerful approach to multiple testing. *J. R. Stat. Soc. B. Met.* **57**, 289–300.
- Buttner, D. (2012) Protein export according to schedule: architecture, assembly, and regulation of type III secretion systems from plant- and animal-pathogenic bacteria. *Microbiol. Mol. Biol. Rev.* **76**, 262–310.
- Buttner, D. and He, S.Y. (2009) Type III protein secretion in plant pathogenic bacteria. *Plant Physiol.* **150**, 1656–1664.
- Casabuono, A., Petrocelli, S., Ottado, J., Orellano, E.G. and Couto, A.S. (2011) Structural analysis and involvement in plant innate immunity of *Xanthomonas axonopodis* pv. *citri* lipopolysaccharide. *J. Biol. Chem.* **286**, 25 628–25 643.
- Cho, K.H. and Caparon, M.G. (2008) tRNA modification by GidA/MnmE is necessary for *Streptococcus pyogenes* virulence: a new strategy to make live attenuated strains. *Infect. Immun.* **76**, 3176–3186.
- Dunger, G., Arabolaza, A., Gottig, N., Orellano, E. and Ottado, J. (2005) Participation of *Xanthomonas axonopodis* pv. *citri* *hrp* cluster in citrus canker and non-host plant responses. *Plant Pathol.* **54**, 781–788.
- Durand, J.M., Dagberg, B., Uhlin, B.E. and Bjork, G.R. (2000) Transfer RNA modification, temperature and DNA superhelicity have a common target in the regulatory network of the virulence of *Shigella flexneri*: the expression of the *virF* gene. *Mol. Microbiol.* **35**, 924–935.
- Galan, J.E., Lara-Tejero, M., Marlovits, T.C. and Wagner, S. (2014) Bacterial type III secretion systems: specialized nanomachines for protein delivery into target cells. *Annu. Rev. Microbiol.* **68**, 415–438.
- Gentleman, R.C., Carey, V.J., Bates, D.M., Bolstad, B., Dettling, M., Dudoit, S., Ellis, B., Gautier, L., Ge, Y. and Gentry, J. (2004) Bioconductor: open software development for computational biology and bioinformatics. *Genome Biol.* **5**, R80.
- Guo, Y., Figueiredo, J.F., Jones, J. and Wang, N. (2011) HrpG, together with HrpX, play global roles in coordinating different virulence traits of *Xanthomonas axonopodis* pv. *citri*. *Mol. Plant-Microbe Interact.* **24**, 649–661.

- Guo, Y., Zhang, Y., Li, J.L. and Wang, N. (2012) Diffusible signal factor-mediated quorum sensing plays a central role in coordinating gene expression of *Xanthomonas citri* subsp. *citri*. *Mol. Plant-Microbe Interact.* **25**, 165.
- Hammond-Kosack, K.E. and Jones, J.D. (1996) Resistance gene-dependent plant defense responses. *Plant Cell*, **8**, 1773–1791.
- Haydon, D.J. and Guest, J.R. (1991) A new family of bacterial regulatory proteins. *FEMS Microbiol. Lett.* **63**, 291–295.
- Hildebrandt, A. and Roots, I. (1975) Reduced nicotinamide adenine dinucleotide phosphate (NADPH)-dependent formation and breakdown of hydrogen peroxide during mixed function oxidation reactions in liver microsomes. *Arch. Biochem. Biophys.* **171**, 385–397.
- Hoskisson, P.A. and Rigali, S. (2009) Chapter 1: variation in form and function of the helix-turn-helix regulators of the GntR superfamily. *Adv. Appl. Microbiol.* **69**, 1–22.
- Kinscherf, T.G. and Willis, D.K. (2002) Global regulation by *gidA* in *Pseudomonas syringae*. *J. Bacteriol.* **184**, 2281–2286.
- Konig, B., Muller, J.J., Lanka, E. and Heinemann, U. (2009) Crystal structure of KorA bound to operator DNA: insight into repressor cooperation in RP4 gene regulation. *Nucleic Acids Res.* **37**, 1915–1924.
- Laia, M., Moreira, L., Dezajacomo, J., Brigati, J., Ferreira, C., Ferro, M., Silva, A., Ferro, J. and Oliveira, J. (2009) New genes of *Xanthomonas citri* subsp. *citri* involved in pathogenesis and adaptation revealed by a transposon-based mutant library. *BMC Microbiol.* **9**, 12.
- Li, H. and Durbin, R. (2009) Fast and accurate short read alignment with Burrows–Wheeler transform. *Bioinformatics*, **25**, 1754–1760.
- Li, J. and Wang, N. (2011) The *wxaco* gene of *Xanthomonas citri* subsp. *citri* encodes a protein with a role in lipopolysaccharide biosynthesis, biofilm formation, stress tolerance and virulence. *Mol. Plant Pathol.* **12**, 381–396.
- Li, R.F., Lu, G.T., Li, L., Su, H.Z., Feng, G.F., Chen, Y., He, Y.Q., Jiang, B.L., Tang, D.J. and Tang, J.L. (2014) Identification of a putative cognate sensor kinase for the two-component response regulator HrpG, a key regulator controlling the expression of the *hrp* genes in *Xanthomonas campestris* pv. *campestris*. *Environ. Microbiol.* **16**, 2053–2071.
- Lin, H.C., Hsu, S.T., Chang, H. and Tzeng, K.C. (2010) A pectate lyase homologue *Pel1* from *Xanthomonas axonopodis* pv. *citri* is associated with the water-soaked margins of canker lesions. *J. Plant Pathol.* **92**, 149–156.
- Litwin, C.M. and Calderwood, S.B. (1993) Role of iron in regulation of virulence genes. *Clin. Microbiol. Rev.* **6**, 137–149.
- Liu, R.J., Zhou, M., Fang, Z.P., Wang, M., Zhou, X.L. and Wang, E.D. (2013) The tRNA recognition mechanism of the minimalist SPOUT methyltransferase, TrmL. *Nucleic Acids Res.* **41**, 7828–7842.
- Livak, K. and Schmittgen, T. (2001) Analysis of relative gene expression data using real-time quantitative PCR and the 2-DeltaDeltaCT method. *Methods*, **25**, 402–408.
- Mahony, S. and Pugh, B.F. (2015) Protein–DNA binding in high-resolution. *Crit. Rev. Biochem. Mol. Biol.* **50**, 269–283.
- Nies, D.H. (2003) Efflux-mediated heavy metal resistance in prokaryotes. *FEMS Microbiol. Rev.* **27**, 313–339.
- Pabo, C.O. and Sauer, R.T. (1992) Transcription factors: structural families and principles of DNA recognition. *Annu. Rev. Biochem.* **61**, 1053–1095.
- Pandey, A. and Sonti, R.V. (2010) Role of the FeoB protein and siderophore in promoting virulence of *Xanthomonas oryzae* pv. *oryzae* on rice. *J. Bacteriol.* **192**, 3187–3203.
- Reja, R., Vinayachandran, V., Ghosh, S. and Pugh, B.F. (2015) Molecular mechanisms of ribosomal protein gene coregulation. *Genes Dev.* **29**, 1942–1954.
- Rhee, H.S. and Pugh, B.F. (2011) Comprehensive genome-wide protein–DNA interactions detected at single-nucleotide resolution. *Cell*, **147**, 1408–1419.
- Rhee, H.S. and Pugh, B.F. (2012) ChIP-exo method for identifying genomic location of DNA-binding proteins with near-single-nucleotide accuracy. *Curr. Protoc. Mol. Biol.* **100**. doi:10.1002/0471142727.mb2124s100.
- Rigali, S., Derouaux, A., Giannotta, F. and Dusart, J. (2002) Subdivision of the helix-turn-helix GntR family of bacterial regulators in the FadR, HutC, MocR, and YtrA subfamilies. *J. Biol. Chem.* **277**, 12 507–12 515.
- Rigano, L., Siciliano, F., Enrique, R., Sendin, L., Filippone, P., Torres, P., Qüesta, J., Dow, J., Castagnaro, A. and Vojnov, A. (2007) Biofilm formation, epiphytic fitness, and canker development in *Xanthomonas axonopodis* pv. *citri*. *Mol. Plant-Microbe Interact.* **20**, 1222–1230.
- Rodionov, D.A. (2007) Comparative genomic reconstruction of transcriptional regulatory networks in bacteria. *Chem. Rev.* **107**, 3467–3497.
- Salzberg, L.I., Luo, Y., Hachmann, A.B., Mascher, T. and Helmann, J.D. (2011) The *Bacillus subtilis* GntR family repressor YtrA responds to cell wall antibiotics. *J. Bacteriol.* **193**, 5793–5801.
- Schwyn, B. and Neilands, J.B. (1987) Universal chemical assay for the detection and determination of siderophores. *Anal. Biochem.* **160**, 47–56.
- Shippy, D.C. and Fadl, A.A. (2015) RNA modification enzymes encoded by the *gid* operon: implications in biology and virulence of bacteria. *Microb. Pathog.* **89**, 100–107.
- Shippy, D.C., Eakley, N.M., Lauhon, C.T., Bochsler, P.N. and Fadl, A.A. (2013) Virulence characteristics of *Salmonella* following deletion of genes encoding the tRNA modification enzymes *GidA* and *MnmE*. *Microb. Pathog.* **57**, 1–9.
- Stahler, F.N., Odenbreit, S., Haas, R., Wilrich, J., Van Vliet, A.H., Kusters, J.G., Kist, M. and Bereswill, S. (2006) The novel *Helicobacter pylori* CznABC metal efflux pump is required for cadmium, zinc, and nickel resistance, urease modulation, and gastric colonization. *Infect. Immun.* **74**, 3845–3852.
- Suvorova, I.A., Korostelev, Y.D. and Gelfand, M.S. (2015) GntR family of bacterial transcription factors and their DNA binding motifs: structure, positioning and co-evolution. *PLoS One*, **10**, e0132618.
- Swarup, S., Yang, Y., Kingsley, M. and Gabriel, D. (1992) An *Xanthomonas citri* pathogenicity gene, *pthA*, pleiotropically encodes gratuitous avirulence on non-hosts. *Mol. Plant-Microbe Interact.* **5**, 204–213.
- Tondo, M.L., Petrocelli, S., Ottado, J. and Orellano, E.G. (2010) The monofunctional catalase *KatE* of *Xanthomonas axonopodis* pv. *citri* is required for full virulence in citrus plants. *PLoS One*, **5**, e10803.
- Venter, H., Mowla, R., Ohene-Agyei, T. and Ma, S. (2015) RND-type drug efflux pumps from Gram-negative bacteria: molecular mechanism and inhibition. *Front. Microbiol.* **6**, 377.
- Vila, J., Marti, S. and Sanchez-Cespedes, J. (2007) Porins, efflux pumps and multidrug resistance in *Acinetobacter baumannii*. *J. Antimicrob. Chemother.* **59**, 1210–1215.
- Vindal, V., Suma, K. and Ranjan, A. (2007) GntR family of regulators in *Mycobacterium smegmatis*: a sequence and structure based characterization. *BMC Genomics*, **8**, 289.
- Yamazaki, A., Hirata, H. and Tsuyumu, S. (2008) Type III regulators HrpG and HrpXct control synthesis of  $\alpha$ -amylase, which is involved in *in planta* multiplication of *Xanthomonas axonopodis* pv. *citri*. *J. Gen. Plant. Pathol.* **74**, 254–257.
- Yan, Q. and Wang, N. (2011) The ColR/ColS two-component system plays multiple roles in the pathogenicity of the citrus canker pathogen *Xanthomonas citri* subsp. *citri*. *J. Bacteriol.* **193**, 1590–1599.
- Yan, Q. and Wang, N. (2012) High-throughput screening and analysis of genes of *Xanthomonas citri* subsp. *citri* involved in citrus canker symptom development. *Mol. Plant-Microbe Interact.* **25**, 69–84.
- Yan, Q., Hu, X. and Wang, N. (2012) The novel virulence-related gene *nlxA* in the lipopolysaccharide cluster of *Xanthomonas citri* ssp. *citri* is involved in the production of lipopolysaccharide and extracellular polysaccharide, motility, biofilm formation and stress resistance. *Mol. Plant. Pathol.* **13**, 923–934.
- Zhou, X., Hu, X., Li, J. and Wang, N. (2015) A novel periplasmic protein, VrpA, contributes to efficient protein secretion by the type III secretion system in *Xanthomonas* spp. *Mol. Plant-Microbe Interact.* **28**, 143–153.

## SUPPORTING INFORMATION

Additional Supporting Information may be found in the online version of this article at the publisher's website:

**Fig. S1** Deletion analysis of YtrA downstream genes. The gene arrangement of *ytrA* and the downstream genes encoding a putative ABC transporter system are shown schematically. The single-headed arrows represent the locations and orientations of the genes. The EZ-Tn5 insertions in the mutant are indicated by inverted triangles. The location of each gene in the *Xanthomonas citri* ssp. *citri* 306 chromosome is indicated by numbers. The function domain was predicted by the SMART program (<http://smart.emblheidelberg.de/>). The relative expression change of the genes is indicated by the log<sub>2</sub> fold change (FC) value (mutant/wild-type, M/WT). The genes *XAC1547*, *XAC1546* and *XAC1545* were individually mutated by in-frame deletion. The locations of the deleted fragments in the



chromosome are shown by the black bars. The pathogenicity of the generated mutants was tested in grapefruit using a bacterial inoculum [around  $10^6$  colony-forming units (cfu)/mL]. The inoculated leaf was photographed at 16 days post-inoculation. The experiment was repeated three times with similar results.

**Fig. S2** Phylogenetic tree of the *ytrA* gene family. The orthologous sequences from related genomes were extracted from the Kyoto Encyclopedia of Genes and Genomes Sequence Similarity Database (KEGG SSDB) database with default parameters. The amino acid sequences of the top 100 hits were selected and aligned using clustalW, and the phylogenetic tree was constructed using MEGA6 with the neighbour-joining method. One thousand bootstrap replicates were made and bootstrap values greater than 50% are shown at each node. The scale bar indicates 5% amino acid sequence divergence.

**Fig. S3** Functional classification of the differentially regulated genes based on the J. Craig Venter Institute (JCVI) database.

**Fig. S4** YtrA is involved in swimming motility on a semi-solid plate (A) and in biofilm formation in a glass tube (B). (A) Swimming motility assay. Bacterial strains were inoculated on a nutrient agar (NA) plate with 0.3% agar with a starting concentration at an optical density at 600 nm ( $OD_{600}$ ) of 0.3. The motility of each strain was monitored by measuring the diameter of the colony edge. The movement of cells was photographed at 4 days post-inoculation. (B) One millilitre of bacterial solution [ $OD_{600} = 0.3$  in nutrient broth (NB)] was incubated at 28 °C for 24 h in a glass tube without shaking. Biofilm formation was visualized by crystal violet staining. The stained cells were dissolved in 97% ethanol and quantified by measuring the  $OD_{590}$  value. The experiments were performed in triplicate and repeated three times with similar results. WT, wild-type strain 306/p53; M, *ytrA* mutant/p53; MC, *ytrA* mutant/p53-YtrA.

**Fig. S5** YtrA controls catalase activity (A) and contributes to resistance against hydrogen peroxide (B). (A) *Xanthomonas citri* ssp. *citri* (*Xac*) strains were cultured for 24 h in plant-mimic medium (XVM2). The crude cell extract was used to test catalase activity. (B) Strains were cultured for 24 h in XVM2. The bacterial population was adjusted to an optical density at 600 nm ( $OD_{600}$ ) of 0.3 and challenged with 20 mM hydrogen peroxide. The living cell population of each strain was examined at different time points. The experiments were performed in triplicate and repeated more than twice with similar results. WT, wild-type strain 306/p53; M, *YtrA* mutant/p53; MC, *ytrA* mutant/p53-YtrA. \*Statistically significant difference between WT and M ( $P < 0.05$ , analysed by Student's two-sample *t*-test).

**Fig. S6** YtrA positively regulates the production of extracellular amylase and cellulase. (A) Extracellular amylase activity assay.

A transparent halo surrounding the colony against the blue background of the plate indicates the secretion of extracellular amylase. (B) Extracellular cellulase activity assay. A transparent halo surrounding the colony against the red background of the plate indicates the secretion of extracellular cellulase. The experiments were performed in triplicate and repeated three times with similar results. WT, wild-type strain 306/p53; M, *ytrA* mutant/p53; MC, *ytrA* mutant/p53-YtrA.

**Fig. S7** YtrA regulates iron uptake in *Xanthomonas citri* ssp. *citri*. (A) Production of siderophore was tested on a chrome-azuroil S-agar (CAS) plate. An orange halo around the colony indicates siderophore production. (B) The mutation of *ytrA* resulted in deficiency in growth under iron-limited conditions. The final concentrations of 2,2'-dipyridyl (DP) are shown. WT, wild-type strain 306/p53; M, *ytrA* mutant/p53; MC, *ytrA* mutant/p53-YtrA.

**Fig. S8** YtrA DNA binding activity is required for bacterial virulence. (A) Protein sequence of the YtrA protein with predicted secondary structure. The helix–turn–helix motif is shown in bold. The conserved residues subjected to mutation are underlined and the mutated residues are shown in red. (B) Pathogenicity assay. Wild-type 306, *ytrA* mutant and *ytrA* mutants expressing YtrA mutations were inoculated on citrus leaves with an initial concentration of  $10^8$  colony-forming units (cfu/mL). Leaves were photographed at 3 days post-inoculation. (C) Detection of expression of YtrA mutation proteins using immunoblotting.

**Fig. S9** Mutation of promoters. (A) Schematic views of the native and mutated promoters selected from *yro* operons with their corresponding length fused with the  $\beta$ -glucuronidase (GUS) reporter gene. (B) Mutations of half-sites of palindromic sequences were confirmed by DNA sequencing. YtrA binding motifs are underlined. Red boxes indicate the mutated nucleotides.

**Fig. S10** Over-expression of *XAC0230* or *XAC0231* does not affect bacterial virulence. (A) Pathogenicity assay. Wild-type 306 harbouring the empty vector, pTF53-czcB, pTF53-0231 and pTF53-0230 were inoculated on citrus leaves with an initial concentration of  $10^8$  colony-forming units (cfu)/mL. Leaves were photographed at 3 days post-inoculation. (B) Detection of protein expression of *XAC0231*, *XAC0230* and CzcB using immunoblotting.

**Fig. S11** Bacterial growth in nutrient broth (NB) medium (A) and plant-mimic medium (XVM2) (B).

**Table S1** Strains and plasmids used in this study.

**Table S2** Primers used in this study (underlining shows the restriction enzyme site).

**Table S3** Summary of DEGs in microarray analysis.

**Table S4** GntR binding motifs of three different operons in multiple bacterial species.